

Point defect creation by swift heavy ion irradiation induced low energy electrons in $YBa_2Cu_3O_{7-y}$

R Biswal¹, J John², D Behera³, P Mallick⁴, Sandeep Kumar⁵, D Kanjilal⁵,
T Mohanty⁶, P Raychaudhuri² and N C Mishra^{1,*}

¹Department of Physics, Utkal University, Bhubaneswar 751004, India

²Tata Institute of Fundamental Research, Mumbai 400005, India

³Department of Physics, National Institute of Technology, Rourkela 769008, India

⁴Department of Physics, North Orissa University, Baripada 757003, India

⁵Inter University Accelerator Center, New Delhi 110067, India

⁶School of Physical Sciences, Jawaharlal Nehru University, New Delhi 110067, India

*E-mail: nareshcmishra@yahoo.co.in

Abstract. The effect of 200 MeV Ag ion irradiation on the superconducting and normal state properties of the high- T_c superconductor $YBa_2Cu_3O_{7-y}$ (YBCO) is studied by in-situ temperature dependent resistance measurement. We show that irradiating YBCO thin films (~ 150 nm) at low temperature result into a softly defected region of about 85 nm radius due to swift heavy ion induced secondary electrons around the highly amorphized latent tracks of ~ 5 nm radius. This leads to decrease of T_c at fluences three orders of magnitude less than the threshold fluence, where overlapping of tracks block supercurrent path. Due to their low energy (4.1 keV for 200 MeV Ag ion), the secondary electrons can induce point defects by inelastic process rather than by direct elastic collision.

PACS number(s): 61.80.Lj, 74.72.Bk, 74.78.Bz, 74.62.-c

1. Introduction

The energy deposited by swift heavy ions (SHI) to the electrons of a target material can reach very high values, some tens of $\text{keV}\cdot\text{nm}^{-1}$. Calculation shows that about half of this energy is deposited in a range of a few nanometers around the ion path, which lead to latent track formation [1, 2]. The remaining energy is transported away by secondary electrons (SE), which are sufficiently energetic to escape the immediate wake of the primary particle and enter a virgin region around the track [3-6]. Only a small fraction of the SE produced may leave the target. Direct experimental evidence of the ejected electrons exist in the literature and a large number of studies have been devoted to determine the number of SE that are emitted per single ion impact, their energy and angular distribution etc [7]. The large fraction of the SE, which are left behind in the solid and dissipate their energy in a region surrounding the ion track mostly cause electronic excitation and ionization leading to scintillation in inorganic media like alkali halides [8].

In the present study, we investigate the evolution of temperature dependent resistance, $R(T)$ of $YBa_2Cu_3O_{7-y}$ (YBCO) thin films measured in-situ with 200 MeV Ag ion irradiation. Contrary to the expectation that the T_c should decrease beyond a threshold fluence where no more continuous superconducting paths exist in the undamaged zones of the grains [9], we show that at very low fluences the T_c decreases when the films are irradiated at low temperature. To explain the unexpected T_c decrease at very low fluences of irradiation, we consider the effect of the SHI induced SE in creating point defects around the ion tracks by inelastic interaction. We thus address a new mode of defect creation by SHI induced SE in addition to the two already established modes of defect creation, namely the electronic and the nuclear energy loss of energetic ions. On the application front, our study reveals that the knowledge of radiation damage

processes due to SHI induced SE in high temperature superconductors is essential, for example, in space satellites where it encounters with energetic cosmic particles, in superconducting magnet of fusion reactors and ion beam processing of superconducting electronic devices. Further, our study opens up a unique way of modifying bulk of the materials at least up to a few micron depths from surface by low energy electrons.

2. Experimental

Sintered YBCO target was prepared by conventional solid-state reaction route. Thin films of YBCO were deposited from this target by pulsed laser deposition technique on single crystal $LaAlO_3$ substrate using KrF Excimer pulsed laser (248nm wavelength) in oxygen atmosphere. The substrate temperature was kept at 790° C. Oxygen pressure was maintained 350 mtorr. The energy density was about 2.6 J cm^{-2} with repetition rate of 10 Hz. The thickness of the film was measured using stylus method on a dektak profilometer. X-ray diffraction shows that the films are c-axis oriented. The films of $\sim 150 \text{ nm}$ were irradiated with $200 \text{ MeV } ^{107}\text{Ag}^{+15}$ ions using the 15 MV tandem pelletron accelerator at the IUAC, New Delhi. Irradiation was done at a slightly off-normal condition to avoid channeling effect. The irradiation fluence, Φ was varied from 1×10^9 ions cm^{-2} to 1.17×10^{13} ions cm^{-2} . Due to experimental limitation in the present study, we could not go to still lower fluence. The fluence was estimated by integrating the charges of ions impinging on the samples kept inside a cylindrical electron suppressor. The ion beam was magnetically scanned over a $1 \times 0.5 \text{ cm}^2$ area covering the complete sample surface for uniform irradiation. The samples were mounted on a copper target ladder using silver paste. To prevent sample heating during irradiation and to acquire in-situ resistance data in the low fluence regime, a low ion beam current (0.03 to 0.1 pA) was maintained.

In-situ temperature dependent resistance, $R(T)$ was measured after irradiating the sample with ion beam at different fluences. The temperature during each irradiation was kept at 82 K

using liquid nitrogen as coolant. $R(T)$ data were taken right after irradiation in heating cycle up to a maximum temperature of 150 K. In these measurements, the sample temperature was thus kept well below room temperature (RT) to avoid annealing of irradiation-induced defects as discussed later. The temperature dependent resistance data was acquired using four-probe technique with a computer controlled data acquisition system. With the voltage resolution of 10^{-7} V of the Nanovoltmeter (Keithley DMM196), a constant current of 1 mA from a current source (Keithley 220) flowing through the samples under current reversal mode gives a resolution 100 μOhm in the measured resistance. This amounts to an error of $\sim 0.001\%$ even at the resistance seen in unirradiated samples above T_c . The temperature controller (Lake Shore Model 340) with Pt100 sensor fixed close to the sample monitored sample temperature during in-situ $R(T)$ measurement with a resolution of ± 0.001 K.

The main problem in the present study is related to the accurate determination of the superconducting transition temperature, T_c and its variation with irradiation fluence. Unambiguous determination of T_c however is difficult in cuprate superconductors due to the presence of fluctuation effects, which round the critical behavior of any observable near T_c [10, 11]. We have used the derivative of the resistance data as a function of temperature $\left(\frac{dR}{dT}\right)$, with T_c defined as the peak position of this derivative as has been done by many [10, 12, 13]

3. Results

Figure 1 shows the evolution of $R(T)$ characteristics of the YBCO thin film with 200 MeV Ag ion irradiation. Superconducting transition was seen up to a fluence of 6.17×10^{12} ions cm^{-2} . Zero resistive state however, could only be achieved above the lowest temperature (82 K) of the target ladder up to a fluence of 1.71×10^{11} ions cm^{-2} . At the highest fluence of 1.17×10^{13} ions cm^{-2} used in the present study, superconductivity is completely destroyed and $R(T)$ showed a

semiconducting behavior (figure 1(a)). Figure 2 shows the fluence dependence of T_c . The inset in figure 2 shows the variation of T_c and T_{c0} in the low fluence regime. Both T_c and T_{c0} continuously decrease with fluence up to 1.71×10^{11} ions cm^{-2} , beyond which T_c increases by ~ 1.1 K in the fluence interval 1.71×10^{11} and 6.71×10^{11} ions cm^{-2} . This fluence range also marked a faster decrease of T_{c0} from 87.8 K to well below 82 K and hence could not be recorded within the minimum temperature of the sample holder. Further increasing fluence (up to 6.17×10^{12} ions cm^{-2}) lead to only a slight decrease of T_c within 0.1 K.

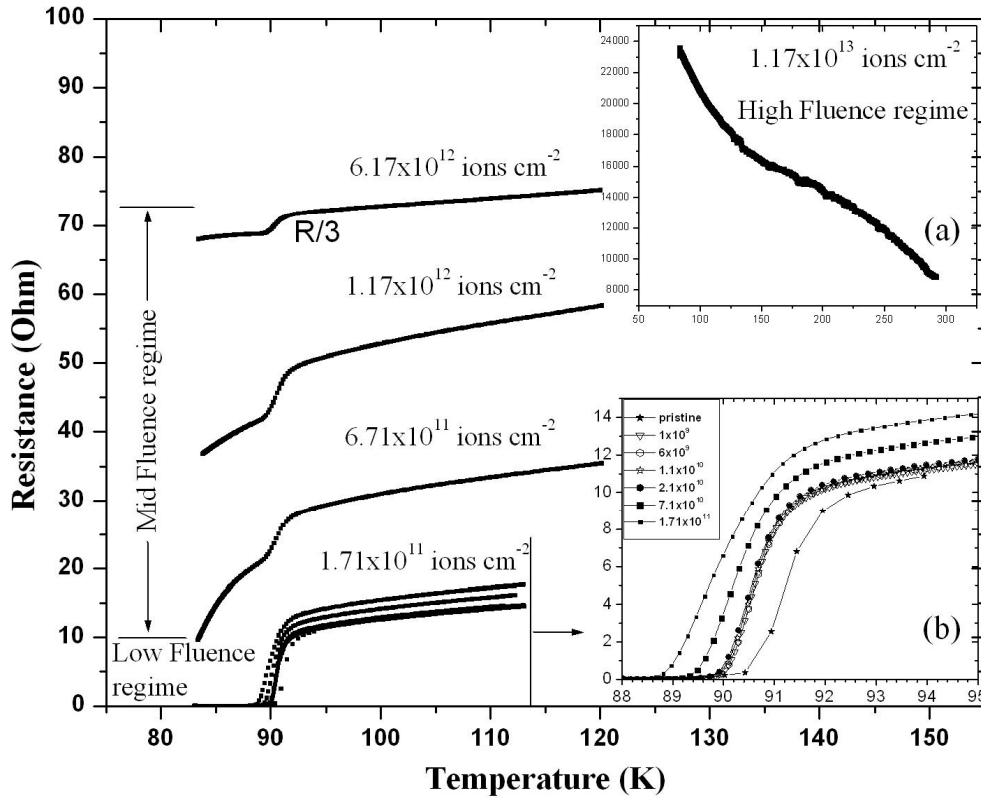


Figure 1. Evolution of superconducting transition with irradiation fluence as probed in-situ through resistance vs. temperature measurement for thin film of $YBa_2Cu_3O_{7-y}$ irradiated at 82 K by 200 MeV Ag ions. Data were taken after each dose of irradiation in the heating cycle up to a maximum of 150 K to avoid annealing of defects. To fit to the scale, the $R(T)$ for the fluence 6.17×10^{12} ions cm^{-2} is divided by 3. Inset (a) shows the temperature dependence of resistance of YBCO films irradiated at a fluence of 1.17×10^{13} ions cm^{-2} . Inset (b) shows the expanded view of the $R(T)$ characteristics in the low fluence regime.

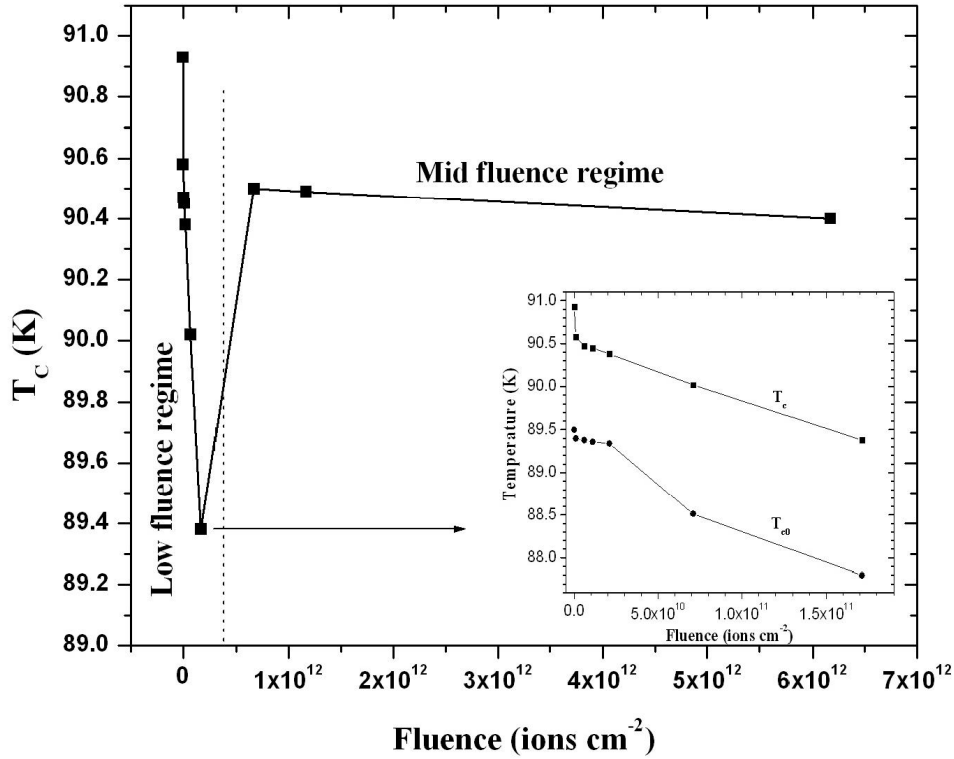


Figure 2. Variation of T_c of $YBa_2Cu_3O_{7-y}$ thin films with 200 MeV Ag irradiation fluence. Inset shows the variation of the T_c and T_{c0} in low fluence regime only.

The evolution of $R(T)$ with irradiation fluence (figure 1) suggests that some differences in the damage mechanisms for different regime of fluences must exist. We define these regimes of fluences as low, mid and high with their characteristic irradiation response. In the low fluence regime, the T_c variation with fluence (figure 2) is not linear. At the first dose (1×10^9 ions cm^{-2}) of irradiation, the T_c decreases at a rate 3.5×10^{-10} K/ ion cm^{-2} . Beyond this fluence T_c decreases at a slower rate of 6.67×10^{-12} K/ion cm^{-2} up to 1.7×10^{11} ions cm^{-2} . The transition from the low fluence to the mid-fluence regime ($1.7 \times 10^{11} \leq \Phi \leq 6.71 \times 10^{11}$ ions cm^{-2}) is marked with a recovery of T_c towards the pristine value and decrease of T_{c0} below 82 K. Increasing fluence in

the mid-fluence regime ($6.71 \times 10^{11} \leq \Phi \leq 6.17 \times 10^{12}$ ions cm^{-2}) causes only a very slight decrease of T_c (within 0.1K). The $R(T)$ in the mid-fluence regime shows a two step transition (figure 1); one at T_c and the other at a lower temperature. In the high fluence regime, the $R(T)$ curve shows semiconducting behaviour. Variation of the resistance normalized at 100 K with temperature for different fluences is shown in figure 3. In spite of the drastic change of superconducting properties and suppression of the T_{c0} , metallic behaviour of $R(T)$ is observed above T_c at all fluences of irradiation except at the highest fluence. The positive value of $\frac{dR}{dT}$ indicating the extent of metallic behaviour, however gradually decreases with increase of irradiation fluence.

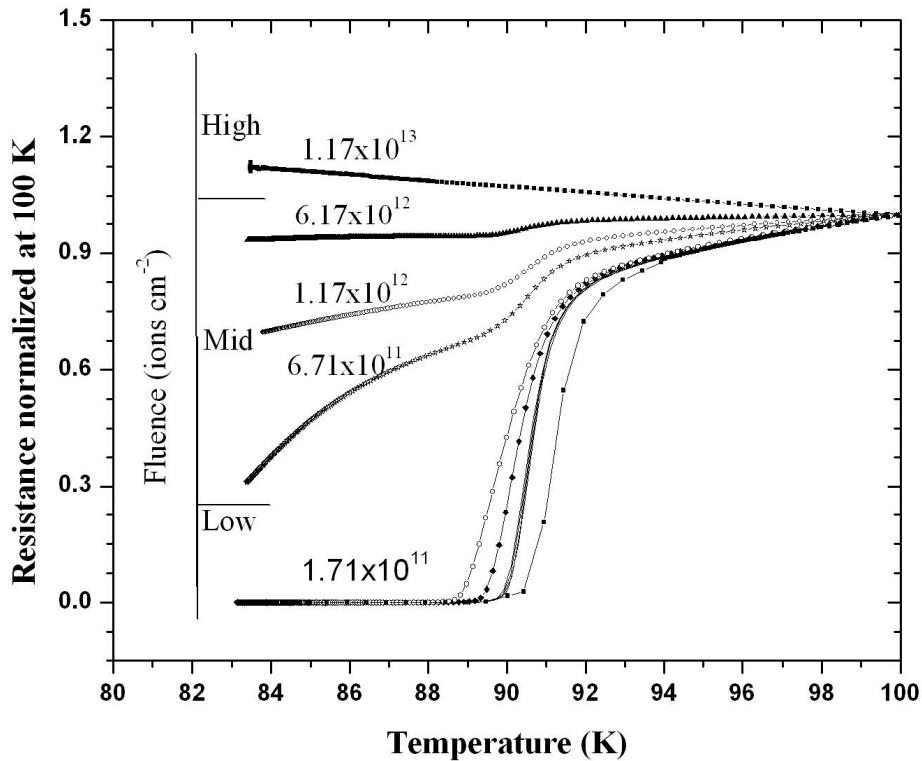


Figure 3. Resistance normalized at 100 K is plotted with temperature for different fluences of irradiation.

4. Discussion

4.1. SHI induce point defects along with latent tracks

The electronic energy loss, S_e , nuclear energy loss, S_n , and range of the 200 MeV Ag ions in YBCO calculated from SRIM 2006 are 25.18 keV nm⁻¹, 70.95 eV nm⁻¹ and 12.66 μ m respectively. Since the thickness of the sample is much less than the range of the ion beam, the energy deposited is uniform along the path of the ion in the film and is mostly due to S_e . The large projectile range also means that the ions are implanted much deeper in the substrate. Since the S_e exceeds the threshold value, S_{eth} (~ 20 keV nm⁻¹) in YBCO [14], these ions create amorphized latent tracks along their trajectory in the films. The tracks of less than 5 nm radius [15] can block supercurrent paths at a fluence $\sim 3 \times 10^{12}$ ions cm⁻² [9]. At a fluence, three order of magnitude lower than this threshold value, only about 0.1% of the sample surface is expected to be covered by latent tracks. The amorphized latent tracks extending from top surface of the film to the film-substrate interface created at 1×10^9 ions cm⁻² cannot account for the observed T_c decrease (3.5×10^{-10} K/ ion cm⁻²) (figure 2), since 99.9% of the YBCO film is still undamaged and can provide percolating supercurrent paths. This unusual result suggests that in addition to latent tracks, there must be a large concentration of other defects created at low temperature by SHI irradiation.

A large number of studies have probed into the effect of SHI irradiation at low temperatures on the superconducting transition through in-situ R(T) measurement in YBCO type superconductors [9, 16-18]. Some of these studies [16-18] have shown that the T_c and the normal state resistivity, which degrade after a dose of irradiation, tend to recover to their pre-irradiation values on annealing the sample at RT. There are several mechanisms proposed for the degradation of these parameters on ion irradiation.

Hensel et al [16] proposed a mechanical stress model to describe the T_c decrease and normal state resistance increase with irradiation fluence. In that model, the amorphized material in the ion induced latent tracks imposes stress in the surrounding crystalline medium of YBCO. As pointed out by these authors, the calculated elongation of the c-axis due to this highly anisotropic strain however is too small to account for the observed T_c decrease. Further, the change of lattice parameter by this mechanical stress is expected to be a permanent, since the amorphized latent tracks once induced do not anneal out at RT. Mechanical stress model [16] therefore cannot account for the observed tendency of T_c and normal state resistance recovery to their pre-irradiation values on increasing the sample temperature to RT. Further, a decrease of T_c due to a very low fluence (10^9 ions cm^{-2}) of irradiation, as observed in the present study where the latent tracks are well separated also rules out the mechanical stress model. Considering the contribution of S_n for defect creation, TRIM simulation for 200 MeV Ag ions in YBCO film gives about 0.04 displacement ion⁻¹ A⁻¹. This gives $\sim 5.2 \times 10^{-8}$ dpa (displacement per atom) for the fluence of 10^9 ions cm^{-2} , which is too small to account for the observed T_c decrease.

Another model [18] considers the SE, which are sufficiently energetic to escape the immediate wake of the primary particle and enter the virgin region of the crystal. The range of the SE can be much larger than the 5 nm radius of ion track. However, unlike the SHI, which create amorphized latent tracks, the SE can induce only point defects. Recovery of T_c and normal state resistivity towards their pre-irradiation values on warming YBCO to RT [16-18] in fact indicate that in addition to amorphized columnar tracks, transient point defects are also created during SHI irradiation.

4.2. Secondary electrons create halo of point defects around latent tracks

The spatial distribution of the energy deposited by SHI in the lattice being dependent on both projectile and target related parameters, a large number of studies have been devoted to estimate

the radial distribution energy, $D(r)$ carried by SE [1, 3-6, 19, 20]. Under the assumption that the SE are ejected normally and their range-energy relation follow power law behavior, Waligorski et al [3] proposed an analytical formulation of $D(r)$ as

$$D(r) = \frac{Ne^4 Z^{*2}}{\alpha m_e c^2 \beta^2 r} \left[\frac{\left(1 - \frac{r+\theta}{R+\theta}\right)^{1/\alpha}}{r+\theta} \right] \quad (1)$$

Where Z^* is the effective charge of the ion moving with a relative velocity $\beta = v/c$ (c is the speed of light) through the medium containing N electrons per cm^3 , m_e is the mass of the electron and θ is the range of an electron with energy corresponding to the ionization potential, which is taken to be 10 eV. The kinematically limited maximum energy of the SE is

$$E_0 = 2m_e c^2 \frac{\beta^2}{1 - \beta^2} \quad (2)$$

For 200 MeV Ag ions, equation (2) gives the maximum energy E_0 of the SE ~ 4.1 keV. All SE of maximum energy E_0 will be contained within a region whose maximum radial extent from the ion tracks corresponds to the range of the electrons. The maximum range of the SE can be well described by the equation [3] $R = kE_0^\alpha$, where $k = 6 \times 10^{-6} \text{ cm}^2 \text{ keV}^{-\alpha}$ and $\alpha = 1.667$ for electrons of energy greater than 1 keV. For 4.1 keV SE in YBCO medium, the maximum radial extent is found to be $6.3 \times 10^{-5} \text{ g cm}^{-2}$, which corresponds to $R \sim 97$ nm. For YBCO,

$\frac{Ne^4}{m_e c^2} = 1.25 \times 10^{-6} \text{ erg cm}^{-1}$ and the effective charge of the 200 MeV Ag ion with an initial

charge state $Z = +15$ is $Z^* = Z \left(1 - \exp\left(-125\beta Z^{-2/3}\right)\right) = 10.88$.

With these values equation (1) gives the radial distribution of the dose deposited by SE in YBCO for 200 MeV Ag^{+15} ions as shown in figure 4. Inclusion of the correction term to the magnitude of $D(r)$ accounting for the missing radial dose in the region of $r = 1 - 10$ nm [3] leads

to the change of the exponent γ in the dependence of deposited dose on radius ($D(r) = r^\gamma$) from -1.3 in the range $0.1 - 1$ nm, to -2.2 in the range $12 - 35$ nm. Beyond $r = 85$ nm, the $D(r)$ decreases rapidly with a γ of -106.7 . Thus the effective range of the SE which can lead to defect creation is not the maximum range of these electrons, but about 10 nm less.

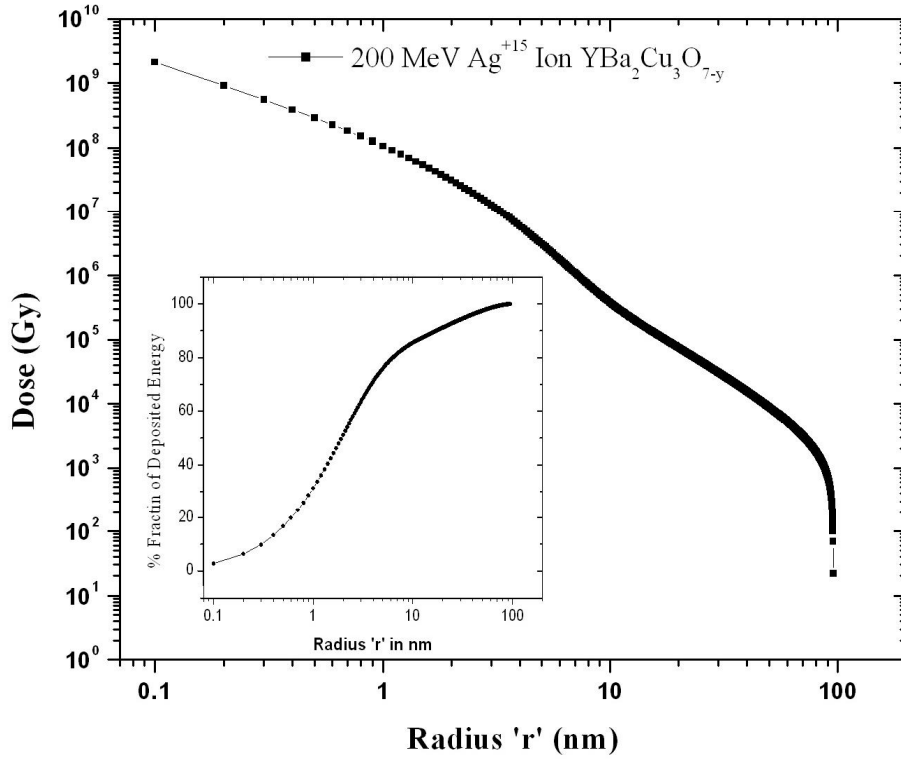


Figure 4. The radial distribution of energy (Dose) around ion path for 200 MeV Ag^{+15} ions in $YBa_2Cu_3O_{7-y}$. The inset shows the fraction of deposited energy carried by secondary electron in cylindrical radius ‘r’ around ion path.

By integrating $D(r)$ in a cylindrical geometry, the fraction of the energy deposited in cylinders of different radii around the ion path is given in the inset of figure 4. This figure shows that about 75% of the energy is deposited within 5 nm from ion path, which is comparable to the

track radius. The rest of the energy is deposited outside the track region with much larger cross section, which can lead to the creation of a halo of point defects as discussed later. Similar halo of defected zone due to SE with diameter ~ 100 to 1000 nm has been seen in polymers [21].

4.3. Defect creation mechanism by low energy secondary electrons

The YBCO structure has two CuO_2 planes per unit cell, where Cu is coordinated to 5 oxygen ions in a pyramidal configuration. There is also one CuO chain per unit cell, where Cu is surrounded by four oxygen ions in square planar configuration. The displacement energy, E_d , per ion for plane and chain oxygen has been found to be 8.4 eV and 2.8 eV, respectively [22]. From the relativistic corpuscular momentum transfer of a two-particle system of electron and oxygen atom in collision, the maximum energy, E_{atom} transferred to the oxygen atom is determined from the equation [23]

$$E_{atom} = 2M \left(E + 2m_e c^2 \right) E / \left[(m_e + M)^2 c^2 + 2M.E \right] \quad (3)$$

Here E is the SE energy, M is the rest mass of the oxygen atom, m_e is that of electron and c is the speed of light. The maximum energy would be transferred with the back scattering angle $\phi = 180^\circ$. Even with low displacement energy (2.8 eV) of the chain oxygen, equation (3) gives the threshold electron energy $E \sim 20$ keV for defect creation in YBCO. Though the molecular dynamics simulation of Cui et al [24] gives an E_d as low as 1.5 eV for chain oxygen displacement, it is still much higher than the calculated E_d of 0.56 eV corresponding to maximum energy (~ 4.1 keV) of the SE induced by 200 MeV Ag^+ ions. The SE therefore cannot account for defect production in YBCO through elastic knock-on process.

To explain the possibilities of defect creation by SHI induced SE, we invoke inelastic interaction of the low energy electrons with the target atoms. Polarized Raman spectroscopy study has also shown inelastic interaction of electrons leading to oxygen rearrangement in YBCO lattice [25]. The energy of the electrons used in that study was 20 keV, which is at the borderline for

inducing defects in YBCO through elastic and inelastic scattering. Our study however deals with SE induced SE with maximum 4.1 keV energy, and hence probes into oxygen rearrangement due to purely inelastic interaction.

Low energy electrons have been shown in the past to break bonds and cause fragmentation of molecules in hydrogen bonded systems and organic medium by a process called dissociative recombination [26]. In inorganic medium, these electrons mostly cause target electron excitation and scintillation as in alkali halides [8]. An inorganic medium like YBCO, however, permits varying oxygen coordination of *Cu* ions in the chains [27] and hence offers an ideal situation for trapping of the SE and consequent oxygen disorder as discussed below.

As oxygen vacancies are created mainly in the *CuO* chains, the oxygen coordination of *Cu* ions next to the vacant oxygen sites is reduced from 4 to 3 or even to 2-fold. *Cu* ion with a 2+ charge state is known to have a minimum of 4-fold oxygen coordination, and in 1+ charge state, it can have a maximum of 2-fold coordination [28]. Therefore, the *Cu* ions with 3-fold oxygen coordination produced due to oxygen vacancies can neither be in 1+ nor in the 2+ charge state. The resulting unstable charge state of these *Cu* ions can fluctuate between two stable charge states 2+ and 1+ with consequent annihilation and creation of holes at the oxygen site [27]. For each oxygen vacancy, there will be two nearby *Cu* ions, which are driven to 3-fold oxygen coordination. In the event, an *Cu* ion in the chains having 3-fold oxygen coordination traps an electron, the unstable charge state of *Cu* will stabilize at 1+. Since in 1+ charge state, *Cu* can have a maximum of 2-fold oxygen coordination, the oxygen in the chains near the trapped electron will be displaced to an interstitial position along a-axis. As a consequence, the SE would induce dissociative recombination by breaking some of the *Cu*–*O* bonds. Such a rearrangement of oxygen configuration in the *CuO* chains can result into shortening of chain length leading to the observed T_c suppression and increase in resistivity even at a fluence much lower than that required for track overlap. The oxygen disorder induced by trapping of the SE is

analogous to that found in photo excitation [29] or 20-keV electron irradiation [25] induced oxygen ordering in the chains. Though SHI induced SE cause T_c decrease, photo-excitation and 20-keV electron irradiation lead to T_c increase in YBCO. In all these cases the influence of the inelastic scattering of incident electrons on the temporal charge imbalance brings about the atomic rearrangements. Further, irradiation with high energy electrons or ions, which create point defects at all atomic sites, particularly at plane oxygen sites lead to a significant and almost linear decrease of T_c with irradiation fluence [30]. On the contrary, whenever defects are created at the CuO chains in the YBCO structure, the T_c is known to decrease non-linearly with defect concentration [27, 31]. The non-linear decrease of T_c with irradiation fluence (figure 2), as observed in our case, thus indicates that SE indeed creates defects in the CuO chains.

The normalized $R(T)$ (figure 3) shows that with increasing irradiation fluence, YBCO is homogeneously defected with a global decrease of T_c in the low fluence regime. This phase collapses into two phases in the mid fluence regime, Phase I with a higher T_c and Phase II with a lower T_c . Not just the transition temperature of the two phases are different, their contribution to the total resistivity in the normal state is also different. The T_c of Phase II seems to decrease rapidly with fluence as compared to Phase I. The origin of Phase II could be due to the rearrangement of point defects after certain threshold defect concentration.

5. Conclusion

In the present study we show a new mode of modification of an inorganic medium like the high- T_c superconductor $YBa_2Cu_3O_{7-y}$ (YBCO) due to SHI induced secondary electrons in addition to the two already established modes - the electronic and the nuclear energy loss. These secondary electrons create point defects in 200 MeV Ag irradiated YBCO thin films by a process analogous to dissociative recombination. By in-situ temperature dependent resistance study, we thus observe a decrease of T_c at low fluences, where the latent tracks are well separated.

Acknowledgements

The authors are thankful to the Pelletron group of IUAC, New Delhi for providing a good quality scanned beam for irradiation. This work is supported by the UFUP funding of IUAC, New Delhi.

References

- [1] Meftah A, Brisard F, Costantini J M, Hage-Ali M, Stoquert J P, Sruder F and Toulemonde M 1993 *Phys. Rev. B* **48** 920
- [2] Furuno S, Otsu H, Hojou K and Izui K 1996 *Nucl. Instr. and Meth. B* **107** 223
- [3] Waligorski M P R, Hamm R N and Katz R 1986 *Nucl. Tracks Radiat. Meas.* **11** 309
- [4] Toulemonde M, Dufour C and Paumier E 1992 *Phys. Rev. B* **46** 14362
- [5] Wang Z G, Dufour C, Cabeau B, Dural J, Fuchs G, Paumier E, Pawlak F and Toulemonde M 1996 *Nucl. Instr. and Meth. B* **107** 175
- [6] Trautmann C, Toulemonde M, Dufour C and Paumier E 1996 *Nucl. Instr. and Meth. B* **108**, 94
- [7] Richter V, Fizgeer B, Michaelson Sh, Hoffman A and Kalish R 2004 *J. Appl. Phys.* **96** 5824 and references therein
- [8] Meyer A and Murray R B 1996 *Phys. Rev.* **128** 98
- [9] Bourgault D, Bouffard S, Toulemonde M, Groult D, Provost J, Studer F, Nguyen N and Raveau B 1989 *Phys. Rev. B* **39** 6549
- [10] Pureur P, Menegotto Costa R, Rodrigues P, Schaf J and Kunzler J V 1993 *Phys. Rev. B* **47** 11420
- [11] Han S H, Eltsev Yu and Rapp O 2000 *Phys. Rev. B* **61** 11776
- [12] Cukauskas E J and Allen L H 1998 *J. Appl. Phys.* **84** 6187

- [13] Aswal D K, Singh A, Sen S, Kaur M, Viswandham C S, Goswami G L and Gupta S K 2002 *J. Phys. Chem. Solids* **63** 1797
- [14] Balanzat E 1989 *Radiat. Eff.* **110** 99
- [15] Zhu Yimei, Cai Z X, Budhani R C, Suenaga M and Welch D O 1993 *Phys. Rev. B* **48** 6436
- [16] Hensel B, Roas B, Henke S, Hopfengartner R, Lippert M, Strobel J P, Vildic M, Saemann-Ischenko G, and Klaumunzer S 1990 *Phys. Rev. B* **42** 4135
- [17] Iwase A, Ishikawa N, Chimi Y, Tsuru K, Wakana H, Michikami O and Kambara T 1998 *Nucl. Instr. and Meth. Phys. Res. B* **146** 557
- [18] Behera D, Mohanty T, Dash S K, Banerjee T, Kanjilal D, Mishra N C 2003 *Radiation Measurements* **36** 125 and references therein
- [19] Katz R and Kobetich E J 1969 *Phys. Rev.* **186** 344
- [20] Fain J, Monin M and Montret M 1974 *Radiat. Res.* **57** 379
- [21] Chatterjee A and Magee J L 1980 *Energy Transfer from Heavy Particles*, Lawrence Berkeley Laboratory Report LBL-112 20/UC-48, p 53
- [22] Tolpygo Sergey K, Lin J -Y, Gurvitch M, Hou S Y and Phillips Julia M 1996 *Phys. Rev. B* **53** 12462
- [23] Goldstein H, Poole C P and Safko J L 2002 *Classical Mechanics*, 3rd ed. (Addison-Wesley, San Francisco)
- [24] Cui F Z, Xie J and Li H D 1992 *Phys. Rev. B* **46** 11182
- [25] Seo H W, Chen Q Y, Iliev M N, Johansen T H, Kolev N, Welp U, Wang C and Chu W – K 2005 *Phys. Rev. B* **72** 052501
- [26] Guberman S L 2001 *Science* **294** 1474
- [27] Mohapatra H P , Behera D, Misra S, Mishra N C and Patnaik K 1993 *J. Supercond.* **6** 359
- [28] Wells A F 1975 *Structural Inorganic Chemistry*, 4th ed. (Clatendon Press, Oxpond)

- [29] Bahrs S, Goni A R, Thomsen C, Maiorov B, Nieva G and Fainstein A 2004 *Phys. Rev. B* **70** 014512 and references therein
- [30] Giapintzakis J, Ginsberg D M, Kirk M A and Ockers S 1994 *Phys. Rev. B* **50** 15967
- [31] Cava R, Batlogg B, Chen C H, Rietman E A, Zahurak S M and Werder D 1987 *Phys. Rev. B* **36** 5719

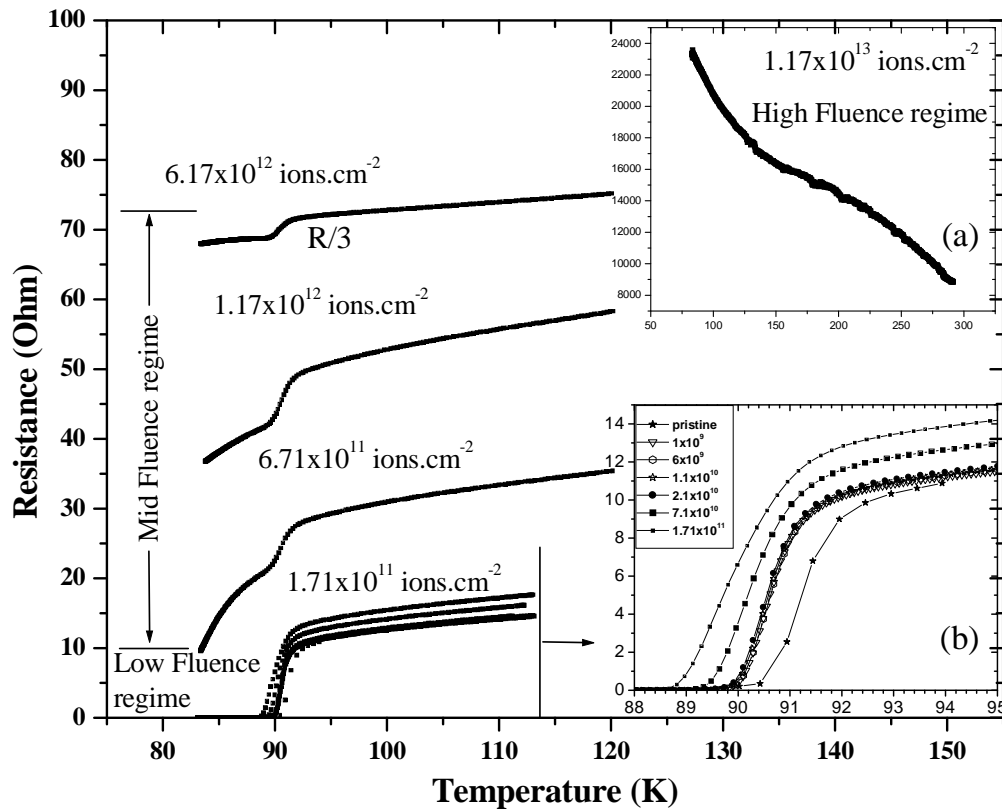


FIG. 1. Evolution of superconducting transition with irradiation fluence as probed through resistance vs. temperature measurement for thin film of $\text{YBa}_2\text{Cu}_3\text{O}_{7-y}$ irradiated

at 82 K by 200 MeV Ag ions. Data were taken after each dose of irradiation in the heating cycle up to a maximum of 150 K to avoid annealing of defects. To fit to the scale, the $R(T)$ for the fluence 6.17×10^{12} ions.cm⁻² is divided by 3. Inset (a) shows the temperature dependence of resistance of YBCO films irradiated at a fluence of 1×10^{13} ions.cm⁻². Inset (b) shows the expanded view of the $R(T)$ characteristics in the low fluence regime.

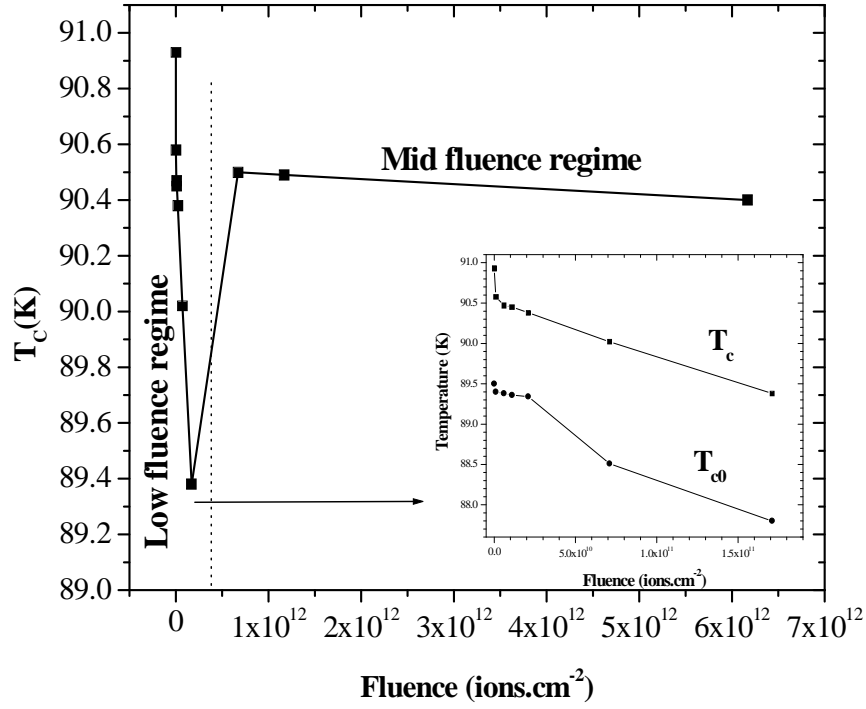


FIG. 2. Variation of the mean field transition temperature, T_c of $YBa_2Cu_3O_{7-y}$ thin films with 200 MeV Ag irradiation fluence. Inset shows the variation of the T_c and T_{c0} in low fluence regime only.

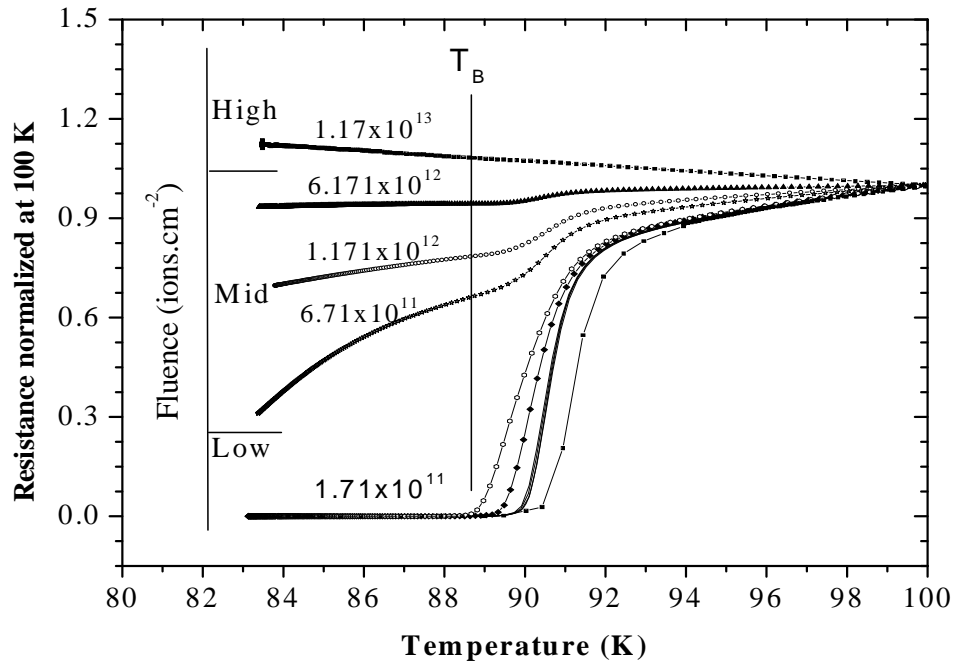


FIG. 3. Resistance normalized at 100 K is plotted with temperature for different fluences of irradiation. T_B (88.7 K) marks the branching of the $R(T)$, where dR/dT is minimum below T_c .

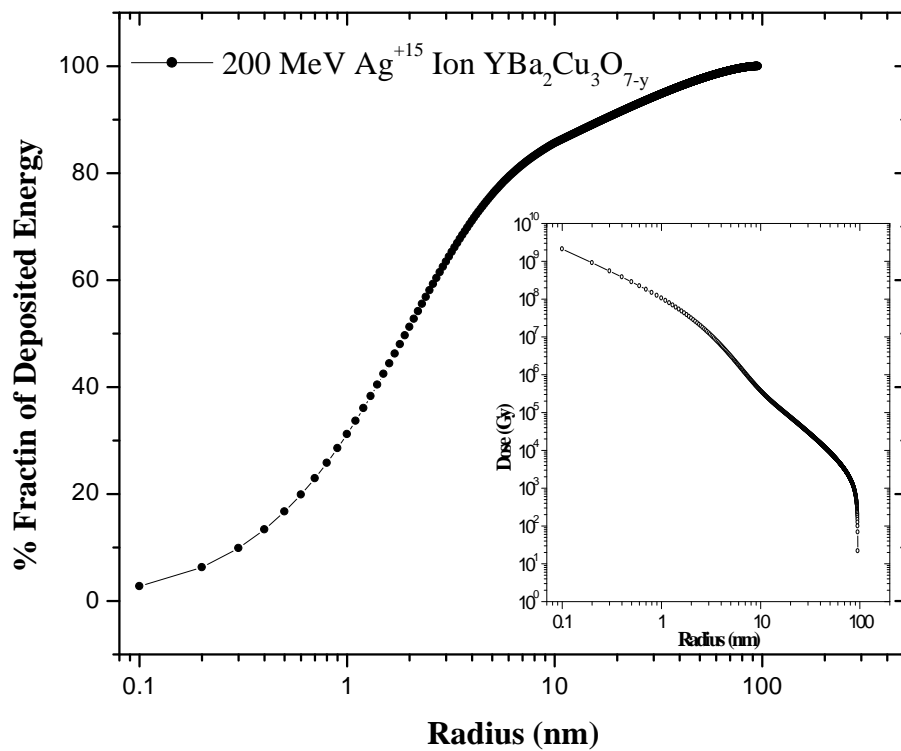


FIG. 4. Fraction of deposited energy carried by secondary electron in cylindrical radius 'R' around ion path vs the cylindrical radius 'R' for 200 MeV Ag^{+15} ion in $\text{YBa}_2\text{Cu}_3\text{O}_{7-y}$. The inset shows the radial distribution of energy (Dose) around ion path.